Origin and Characteristics of Preferential Adsorption on Different Sites in Cobalt-Exchanged Ferrierite

Scott A. McMillan, Randall Q. Snurr, and Linda J. Broadbelt*

Department of Chemical Engineering, 2145 Sheridan Road, Northwestern University, Evanston, Illinois 60208-3120

Received: June 17, 2003; In Final Form: September 29, 2003

The catalytic activity of metal-exchanged zeolites for nitrogen oxide (NO_x) reduction in the literature, as measured by the turnover of individual metal atoms, is not constant but generally increases with metal loading. The occupation of specific zeolite environments by metal atoms is also a function of the metal loading, suggesting that the metal−zeolite coordination environment influences the observed catalytic activity. Here, first principles calculations were applied to examine the adsorption of several molecules relevant to de-NO_x catalysis for two metal−zeolite environments. For a given adsorbate, the preference for cobalt in the ferrierite B environment over the G environment ranges from negligible to approximately 40 kJ/mol. Two primary characteristics were identified that account for the variable preferential adsorption. First, calculations revealed that cobalt in the B environment is more coordinatively unsaturated than cobalt in the G environment. The second characteristic arises from the adsorbate-induced strain on the local zeolite environments, which is generally larger for the G environment. Additional effects are discussed for molecules capable of forming secondary hydrogen bonds with the zeolite and/or highly polar molecules such as water.

Introduction

Metal-exchanged zeolites are active catalysts for the selective catalytic reduction (SCR) of nitrogen oxides (NO_x) with hydrocarbons.[1] Cobalt-exchanged zeolites are particularly notable for their high SCR activity.[2,3] An interesting feature of hydrocarbon SCR over cobalt−zeolites is that the SCR activity depends on the cobalt loading.[4] The turnover of NO to N_2 per cobalt atom is not constant, but rather increases with the amount of cobalt exchanged. This observation may originate from one or more of the following: (1) multiple types of cobalt species are present, (2) the SCR mechanism is enhanced by a synergistic cooperation between nearby cobalt atoms, (3) the accessibility of reactants to cobalt depends on its location in the zeolite channels, and/or (4) the cobalt coordination environment affects the SCR activity.

Careful preparation and characterization of cobalt−zeolites have partially discriminated among these possibilities.[4] Li and Armor[4] used aqueous ion exchange to prepare their cobalt−ferrierite catalysts. Magnetic susceptibility data showed that cobalt was predominantly exchanged in the +2 oxidation state.[5] Sachtler and co-workers carefully characterized cobalt-exchanged MFI prepared under similar exchange conditions. They concluded that cobalt cations prepared by aqueous ion exchange are primarily isolated high-spin cations coordinated only to the zeolite framework.[6−8] These results strongly suggest that only one type of cobalt species, isolated high-spin Co^{2+}, was present in the catalyst examined by Li and Armor.[4]

At very low cobalt loadings (Co/Al < 0.1), the SCR activity has been correlated to the occupation of specific extraframework sites.[9] For example, cobalt occupies three sites in ferrierite:[10] the B, C, and G extraframework sites in the notation of Mortier.[11] The SCR activity of cobalt−ferrierite at low loadings follows the same trend as the relative cobalt occupation of the B site. The smallest distance between any pair of sites is the B−B distance. Kaucký et al.[9] observed similar behavior for other zeolites in addition to ferrierite: the most active cobalt site for a given zeolite topology corresponded to the sites with the smallest separation distance between the sites. On the basis of these results, Kaucký et al.[9] suggested that the SCR activity is enhanced by a synergistic cooperation between nearby cobalt cations. Since the probability of nearby cobalt cations increases with the cobalt loading, the turnover frequency should also increase according to the synergistic mechanism.

Cobalt in the ferrierite B site should also be the most accessible to reactant molecules; the B site is located at the wall of the 10-membered-ring channel near the intersection of the 10-membered- and eight-membered-ring channels, while the G site is located in the smaller eight-membered-ring channels. The C site is even less accessible and is only sparsely populated by cobalt.[10] For ferrierite, the most accessible site was also the most active at low loadings;[9] however, for other zeolites, the most active site did not necessarily correspond to the most accessible site. This suggests that the zeolite channels are sufficiently large so that diffusion effects are not significant.

The influence of the zeolite coordination environment on SCR activity is largely unknown. While inferences can be made based on the experimental data, the isolation of individual sites is necessary to fully characterize this effect. Exchanging cobalt in only one particular extraframework site is an extremely difficult, if not impossible, task. Theoretical calculations can contribute here based on their ability to investigate individual environments easily. However, most theoretical investigations have focused on only one metal−zeolite exchange environment at a time (e.g., refs 12−14). Other calculations have demonstrated that characteristics of bare metal-exchanged zeolites, such as the EPR signal or infrared spectrum, depend on the coordination environment (e.g., refs 15−18). However, only a

* Corresponding author. Phone: 847-491-5351. E-mail: broadbelt@northwestern.edu.

10.1021/jp0357166 CCC: $25.00
Published on Web 11/06/2003

few reports have suggested how the local zeolite environment may affect the adsorption of molecules, which is presumably closely related to the catalytic activity. Van Santen and co-workers[19−21] demonstrated that the adsorption of molecular hydrogen, water, and methane depends on the zinc−zeolite coordination environment. They suggested that differences in the extent of the weakening of zinc−zeolite bonds may explain the differences in the adsorption energies. Previously, we proposed and quantified two adsorption properties that account for the calculated ∼50 kJ/mol difference in the adsorption energy of NO to cobalt in the B and G ferrierite sites.[22] Approximately 40% of the difference is due to intrinsic factors, i.e., cobalt is more coordinatively unsaturated in the B site than the G site. The remaining difference in the adsorption energy was shown to arise from adsorption-induced strain on the metal−zeolite; cobalt in the G site must adopt a more highly strained position to adsorb NO than cobalt in the B site. Davidová et al.[23] also found that the adsorbate-induced strain on the local zeolite environment was more significant for some copper−zeolite environments than others. Here, these two factors are further investigated for other molecules relevant to lean-burn emissions treatment. In particular, we examine the adsorption properties as a function of the cobalt−zeolite environment to determine if these two factors more generally control molecular adsorption heterogeneity. The selected molecules encompass a wide range of gas-phase chemical properties (i.e., no dipole (N_2), a small dipole (NO), and a large dipole (NH_3)) to critically examine the effects of strain and coordinative unsaturation.

Computational Methods

Cobalt primarily occupies the B and G sites in ferrierite.[10,24] Since cobalt is divalent, at least two framework aluminum atoms must be located near these exchange sites. The agreement between calculated properties and experimental data suggests that the 1,4 arrangement of aluminum atoms in the B site and the 1,3 arrangement in the G site are the most probable environments for cobalt,[18] where 1, 3, and 4 refer to the T atom positions in the 6-ring of the B and G sites, as shown in Figure 1. While examining the interaction of NO with cobalt in the B and G sites, we considered all of the possible aluminum arrangements in both of these sites.[22] While minor differences were observed between different aluminum arrangements in a given site, these differences were small compared to the overall difference between the B and G sites. Hence, here we only consider the B-1,4 and G-1,3 cobalt environments even though these are just two of the possible environments and no definitive evidence shows that these particular environments are predominant over any of the others.

Zeolite clusters corresponding to the B-1,4 and G-1,3 environments were extracted from the ferrierite framework. Figure 1 shows the two clusters interacting with an adsorbed carbon monoxide molecule. The atoms at the edge of each cluster were terminated by hydrogen atoms directed along the bond vector of what would have been the next zeolite framework atom; the hydrogen atoms are not shown in any of the cluster illustrations (e.g., Figure 1). The Si−H and O−H distances were fixed at 1.49 and 0.98 Å, respectively. The Cartesian positions of the terminating OH and SiH_3 groups were constrained while the rest of the cluster and the adsorbate molecule were allowed to relax fully; the unconstrained part of the clusters includes, but is not limited to, the entire six-membered ring of both sites. The optimized structures of the two environments were calculated with use of the Gaussian 98 software package.[25] The BP86 density functional and LANL2DZ basis set were used in all of the calculations. Wave function stability calculations confirmed the ground-state configuration of all the wave functions. Frequency calculations using a modified Hessian eigenvalue method[18,22] were performed to ensure that the optimized geometries corresponded to minimum energy structures on the constrained potential energy surface.

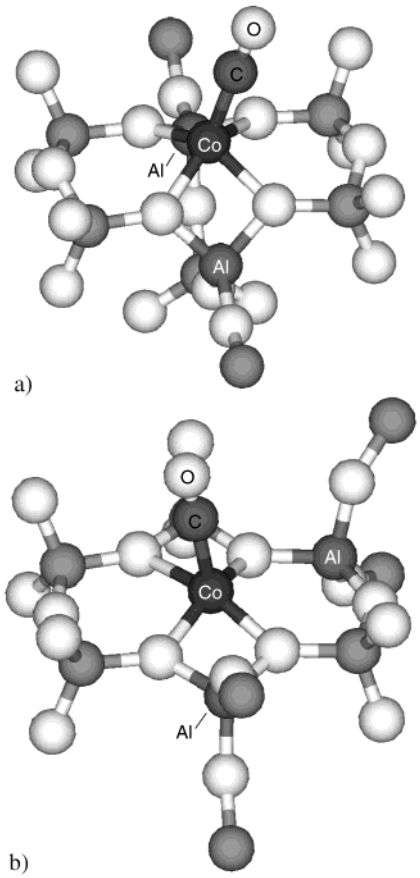

Figure 1. Adsorption of carbon monoxide on cobalt (Co−CO) in the (a) B-1,4 and (b) G-1,3 environments (terminating hydrogen atoms not shown). Unless otherwise denoted, oxygen atoms are shown in light gray and silicon atoms are shown in dark gray.

Results and Discussion

NO adsorption on these two cobalt−ferrierite environments was investigated previously.[22] Here, molecular adsorption properties were calculated for carbon monoxide (CO), dinitrogen (N_2), nitrous oxide (N_2O), nitrogen dioxide (NO_2), ammonia (NH_3), and water (H_2O); the ammonia and water results will be discussed later in a separate subsection. The calculated adsorbate structures corresponding to specific configurations are shown for CO, O-down N_2O, and N-down NO_2 in Figures 1, 2, and 3, respectively. For any given adsorbate molecule, the adsorbate structure may differ between the B-1,4 and G-1,3 environments. For example, the Co−N−O angle is linear for the B-1,4 environment, but is bent for the G-1,3 environment.[22] We previously explained this difference in terms of the relative position of the antibonding d_{zz} band. Not all of the adsorbates have such distinctive structural differences; for example, nitrous oxide adsorbed in the O-down configuration has a similar structure for both environments (Figure 2). However, these structural features are not the focus of this work and will be discussed further only as necessary to address other adsorption properties.

The overlap of atomic orbitals centered on one atom with those centered on another atom projected onto the density of

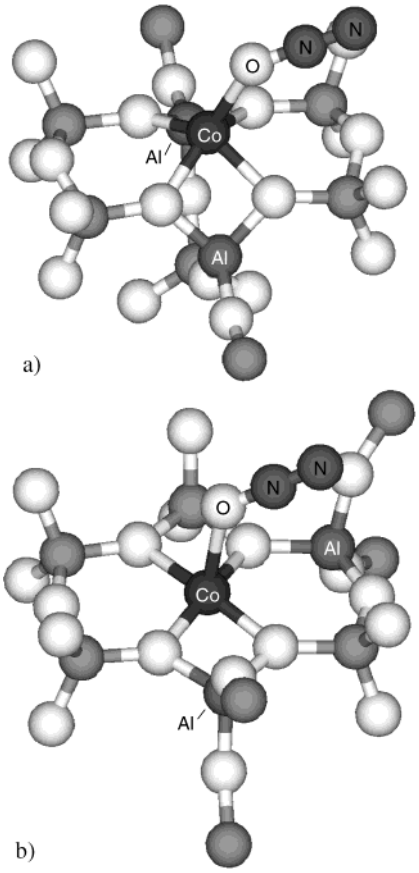

Figure 2. Adsorption of nitrous oxide in the O-down configuration on cobalt ($Co-ON_2$) in the (a) B-1,4 and (b) G-1,3 environments (terminating hydrogen atoms are not shown).

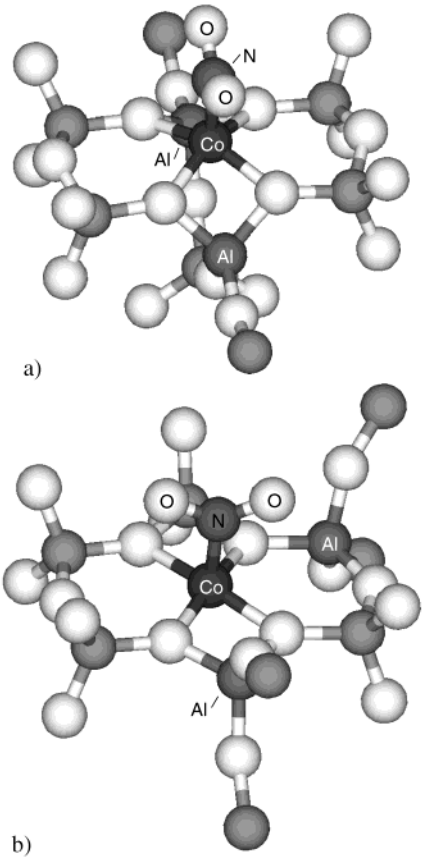

Figure 3. Adsorption of nitrogen dioxide in the N-down configuration on cobalt ($Co-NO_2$) in the (a) B-1,4 and (b) G-1,3 environments (terminating hydrogen atoms are not shown).

states is known as the molecular orbital overlap population (MOOP).[26] Unlike the density of states, the MOOP may be positive (bonding interactions), zero (nonbonding), or negative (antibonding interactions); the relative magnitude indicates the degree of interaction. For all of these molecules, the interaction between the cobalt−ferrierite environment and the adsorbate occurs primarily between cobalt and the nearest adsorbate atom. The MOOP between this adsorbate atom and cobalt is significantly larger than any of the other adsorbate/cobalt−zeolite overlap populations.

Several spin states are possible and must be considered in detail. Some of the gas-phase molecules possess unpaired electrons: NO and NO_2 each have a single unpaired electron and have the doublet spin state. In all cases, the lowest energy spin states for each component were used to calculate the adsorption energy. The lowest energy spin state for the bare cobalt−zeolite environments was always the quartet state,[18] in agreement with experiment.[6] Multiple spin states were explored for the adsorption complexes; for instance, singlet, triplet, and quintet spin states were each individually optimized for adsorbed NO_2. For all of the adsorbates the spin states with the lowest energy were the same for both environments.

Adsorption Energy. For each molecule, the adsorption energy was calculated according to the chemical reaction:

$$(Z-Co)_i + X \xrightarrow{\Delta E_{ads}} Z-Co-X \qquad (1)$$

where $(Z-Co)_i$ is the optimized structure of the bare cobalt−ferrierite environment, X is the optimized gas-phase molecule, and Z−Co−X is the optimized structure of the adsorption complex. The calculated adsorption energies for all of the molecules are listed in Tables 1 and 2 for the B-1,4 and G-1,3 environments, respectively.

TABLE 1: Calculated B-1,4 Molecular Adsorption Energies (kJ/mol)[a]

	spin[b]	ΔE_{ads}	ΔE_{bond}	ΔE_{strain}	ΔE_{cvp}	$\Delta E_{Coulomb}$
Co−CO	quartet	−103	−111	9	5	−3
$Co-N_2$	quartet	−57	−64	6	3	−3
Co−NO	triplet	−167	−175	8	6	1
Co−ON	triplet	−73	−79	5	0	−11
$Co-N_2O$	quartet	−49	−54	5	3	−3
$Co-ON_2$	quartet	−38	−42	4	1	−21
$Co-NO_2$	singlet	−82	−103	21	9	9
Co−ONO	triplet	−71	−81	10	0	−5

[a] The values correspond to the SCF energy difference. In some cases, the sum of ΔE_{bond} and ΔE_{strain} may not exactly equal ΔE_{ads} due to rounding errors. [b] Overall spin state of adsorbed configuration.

TABLE 2: Calculated G-1,3 Molecular Adsorption Energies (kJ/mol)[a]

	spin[b]	ΔE_{ads}	ΔE_{bond}	ΔE_{strain}	ΔE_{cvp}	$\Delta E_{Coulomb}$
Co−CO	quartet	−72	−99	26	18	−11
$Co-N_2$	quartet	−34	−51	17	11	−10
Co−NO	triplet	−130	−162	32	22	−7
Co−ON	triplet	−43	−62	19	13	−13
$Co-N_2O$	quartet	−29	−44	14	10	−10
$Co-ON_2$	quartet	−18	−26	8	4	−29
$Co-NO_2$	singlet	−78	−91	13	2	9
Co−ONO	triplet	−49	−66	17	9	−2

[a] The values correspond to the SCF energy difference. In some cases, the sum of ΔE_{bond} and ΔE_{strain} may not exactly equal ΔE_{ads} due to rounding errors. [b] Overall spin state of adsorbed configuration.

Table 3 shows the differences in the adsorption energy between the B-1,4 and G-1,3 environments. Adsorption is

TABLE 3: Difference of G-1,3 and B-1,4 Molecular Adsorption Energies (kJ/mol)[a]

	$\Delta(\Delta E_{ads})$	$\Delta(\Delta E_{bond})$	$\Delta(\Delta E_{strain})$
Co−CO	31	12	17
Co−N_2	23	13	11
Co−NO	37	13	24
Co−ON	30	17	14
Co−N_2O	20	10	9
Co−ON_2	20	16	4
Co−NO_2	4	12	−8
Co−ONO	22	15	7

[a] In some cases, the sum of $\Delta(\Delta E_{bond})$ and $\Delta(\Delta E_{strain})$ may not exactly equal $\Delta(\Delta E_{ads})$ due to rounding errors.

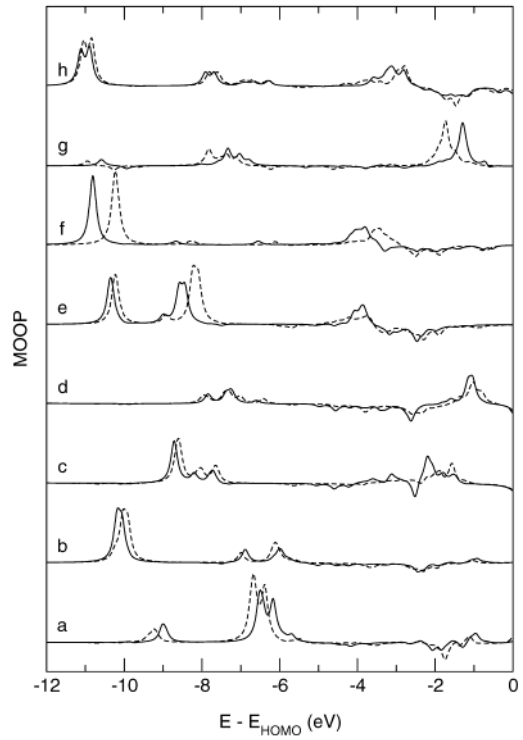

Figure 4. Molecular orbital overlap populations (MOOP) for cobalt in the B-1,4 (solid) and G-1,3 (dashed) environments and the bonded adsorbate atom for (a) Co−CO, (b) Co−N_2, (c) Co−NO, (d) Co−ON, (e) Co−N_2O, (f) Co−ON_2, (g) Co−NO_2, and (h) Co−ONO.

always favored on the B-1,4 environment over the G-1,3 environment, but the degree of this preference varies. NO adsorbed in the N-down configuration has the largest difference, 37 kJ/mol, while NO_2 adsorbed in the N-down configuration shows essentially no adsorption preference. Several features of the electronic structure were examined to determine if different adsorbate bond formation mechanisms were occurring on the two cobalt environments. For a given adsorbate, the Mulliken and Natural Orbital populations were very similar in both environments. Figure 4 shows that the MOOP for cobalt and the adsorbate atom that is directly coordinated to cobalt is very similar regardless of the environment. Hence, the differences in the overall adsorption energy cannot be explained by different cobalt−adsorbate orbital interactions for the two environments.

We previously identified two factors to explain the preference of NO for the B environment over the G environment.[22] Cobalt in the B environment is more coordinatively unsaturated than cobalt in the G environment. Because the degree of coordinative unsaturation is an inherent property of the bare cobalt−zeolite, this contribution would at least partially account for a preference for the B-1,4 environment for all the adsorbates. In addition, the strain that NO induced on the G environment upon adsorption was more significant than that in the B environment. These factors will be explored in the next subsection to determine if they can also explain the variation in the adsorption energies of the other molecules.

Bond and Strain Energy. To evaluate the relative importance of coodinative unsaturation and strain, the overall adsorption energy was decomposed into two energies:

$$(Z-Co)_i + X \xrightarrow{\Delta E_{strain}} (Z-Co)_f + X \quad (2)$$

$$(Z-Co)_f + X \xrightarrow{\Delta E_{bond}} (Z-Co-X) \quad (3)$$

where $(Z-Co)_f$ is the structure of the optimized adsorption complex without the adsorbate and the other terms are unchanged from eq 1. Hence, the strain energy accounts for the change in the atomic positions of the cobalt−zeolite that occur upon adsorption but without the formation of the cobalt−adsorbate bond. Conversely, the bond energy includes only the formation of the cobalt−adsorbate bond; no change in the cobalt−zeolite geometry occurs for this reaction. These reactions are constructed such that:

$$\Delta E_{ads} = \Delta E_{bond} + \Delta E_{strain} \quad (4)$$

The strain energy should always be positive. Prior to adsorption, the atoms of the cobalt−zeolite are in their minimum energy positions. Any displacement from these positions without the formation of a chemical bond will necessarily increase the electronic energy. Consequently, the bond energy must always be less than the adsorption energy. The values of the bond and strain energies are listed in Tables 1 and 2. The differences in the bond and strain energies between the B and G environments for each adsorbate are given in Table 3.

Cobalt Coordinative Unsaturation. Within the accuracy of the calculations, the bond energy preference for the B-1,4 environment is essentially constant. $\Delta(\Delta E_{bond})$ varies from 10 to 17 kJ/mol and has an average value of ∼13 kJ/mol. Formally, cobalt in both environments is coordinated to four framework oxygen atoms. However, the relative strength of these bonds is not necessarily equivalent. The electronic coordination number[27] was determined by using the orbital overlap populations for cobalt without any adsorbates. Cobalt in the B-1,4 environment has a coordination number of 4.2, while cobalt in the G-1,3 environment has a coordination number of 4.6.[22] Hence, adsorption should generally be favored for the B-1,4 environment over the G-1,3 environment since cobalt in the former environment is more coordinatively unsaturated. The calculated differences in the bond energy show that once strain effects are removed, this intrinsic preference for the B-1,4 environment is constant, regardless of the adsorbate or its orientation.

Cobalt−Zeolite Strain. Unlike the bond energy, the strain energy differences between the two environments are not constant as the adsorbate is varied (Table 3); the values of $\Delta(\Delta E_{strain})$ vary from −8 kJ/mol to 24 kJ/mol. With the exception of NO_2 in the N-down orientation, the strain energy is always larger for the G-1,3 environment, i.e., $\Delta(\Delta E_{strain})$ is positive. Prior to adsorption, cobalt in the G-1,3 environment lies in the planar six-membered zeolite ring. Cobalt in the B-1,4 environment is located at the apex of a pyramid formed by cobalt and the four zeolite oxygens to which it is directly coordinated. Cobalt in the G-1,3 environment is displaced by 0.18−0.52 Å depending on the adsorbate, while the displacement in the B-1,4 environment ranges from 0.03 to 0.16 Å. The only exception to this trend is the N-down orientation of NO_2. Rather than

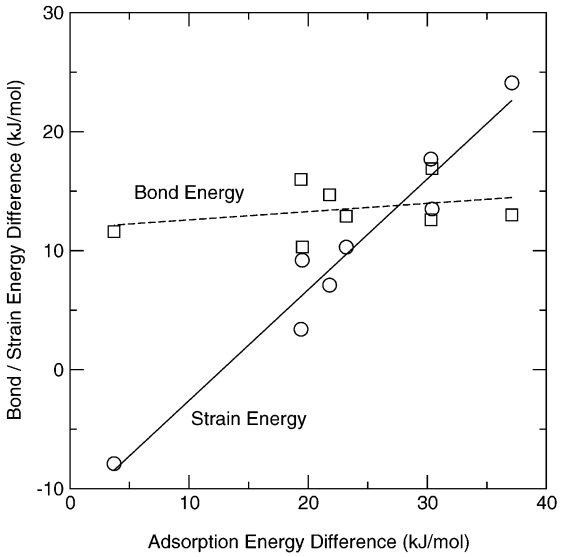

Figure 5. Trends in the difference of the bond (□) and strain (○) energies for the B-1,4 and G-1,3 environments compared to the total difference in the adsorption energies.

pulling cobalt away from the zeolite, NO_2 pushes cobalt 0.21 Å toward the zeolite in the B-1,4 environment, the only situation where this occurs. NO_2 in the N-down orientation is also the only case where the strain is larger for the B-1,4 environment than for the G-1,3 environment.

For NO adsorption, a large fraction of the strain energy was attributed to the cobalt vertical position (CVP).[22] For the other adsorbates, the cobalt vertical displacement is also generally a large fraction of the total zeolite strain (Tables 1 and 2). The non-CVP fraction of the strain energy arises from the combination of many small structural changes. No other single specific structural feature could be identified as dominating the remaining strain energy.

Characteristics of Preferential Molecular Adsorption on Cobalt−Zeolites. The preceding subsections demonstrate that the difference in the bond energy for the two sites is relatively constant regardless of the adsorbate, while the difference in adsorbate-induced strain is highly variable. The overall difference in the adsorption energies for the two environments is a sum of the individual bond and strain energy differences. The bond and strain energy differences are plotted versus the adsorption energy difference in Figure 5. The N-down orientation of NO is located on the far right of the figure. The intrinsic ∼13 kJ/mol bond energy difference is supplemented by a large strain energy difference resulting in an even larger preference for NO adsorption on the B-1,4 environment. At the far left of the figure, NO_2 in the N-down orientation is plotted. The strain energy difference is negative here; the intrinsic preference for the B-1,4 environment is mostly mitigated by the strain energy. Hence, the general characteristic of adsorption energy differences between the two environments is a constant intrinsic preference for the B-1,4 environment due to the relative coordinative unsaturation of cobalt and a variable effect that depends on the adsorbate-induced strain. The cobalt−zeolite strain generally enhances the intrinsic preference, but in some cases may have the opposite effect.

Ammonia and Water. The adsorption of water and ammonia was also investigated. These adsorption energies are reported in Table 4. The adsorbate-induced strain is again more significant for the G-1,3 environment. Unlike the other adsorbates, the intrinsic ∼13 kJ/mol preference (ΔE_{bond}) for the B-1,4 environment is not observed for these two adsorbates; instead,

TABLE 4: Calculated Ammonia and Water Molecular Adsorption Energies (kJ/mol)[a]

	environment	ΔE_{ads}	ΔE_{bond}	ΔE_{strain}	$\Delta E_{Coulomb}$
Co−NH_3	B-1,4	−159	−173	13	−63
Co−NH_3	G-1,3	−143	−178	36	−106
Co−NH_3	G-1,3f	−139	−165	26	−86
Co−OH_2	B-1,4	−126	−139	12	−60
Co−OH_2	G-1,3	−129	−178	49	−134
Co−OH_2	G-1,3f	−116	−142	26	−91

[a] The overall adsorbed spin state is a quartet in all cases.

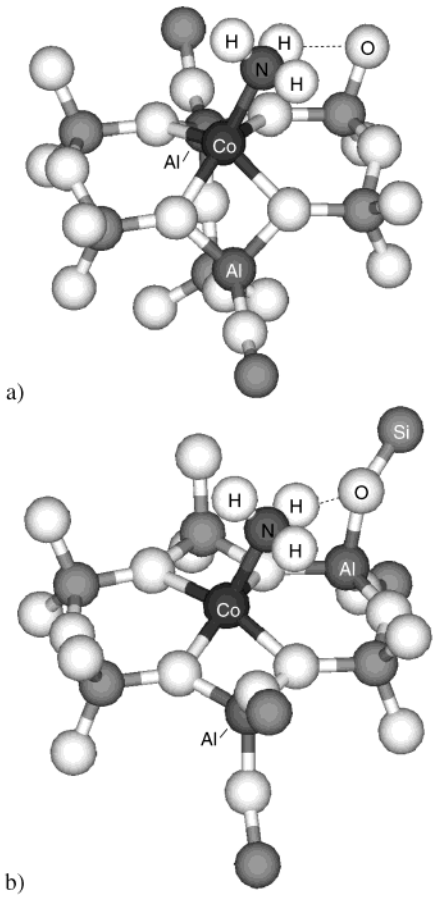

Figure 6. Adsorption of ammonia on cobalt (Co−NH_3) in the (a) B-1,4 and (b) G-1,3 environments (terminating hydrogen atoms not shown). Hydrogen bonds are shown with thin lines. The O−H hydrogen bond distances are 2.84 and 2.23 Å for the B-1,4 and G-1,3 environments, respectively.

the bond energy for the G-1,3 environment is more negative. The calculated ammonia and water adsorption energies deviate from the trend illustrated in Figure 5. However, ammonia and water differ from the other adsorbates investigated here in two important respects, suggesting that additional factors not considered previously may also contribute to preferential adsorption.

The first difference is that these two molecules each form a hydrogen bond with one of the zeolite oxygen atoms as shown in Figures 6 and 7. However, the ability of the zeolite environments to form hydrogen bonds differs. The zeolite oxygen atom involved in the hydrogen bond is fixed in the B-1,4 cluster, but it is flexible in the G-1,3 cluster; the oxygen atom is part of a fixed terminating OH group in the B-1,4 cluster.

To examine the influence of these termination effects, we performed calculations on variations of the B-1,4 and G-1,3 cluster models. The B-1,4 cluster was expanded to include an $OSiH_3$ group in place of the OH terminating group involved in

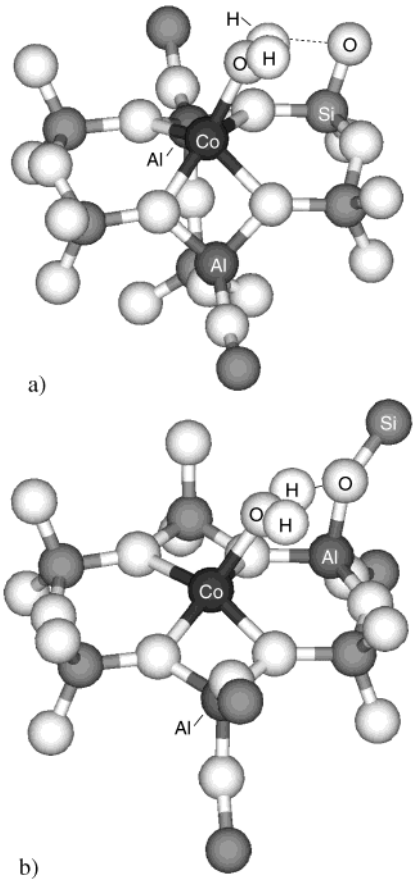

Figure 7. Adsorption of water on cobalt ($Co-OH_2$) in the (a) B-1,4 and (b) G-1,3 environments (terminating hydrogen atoms are not shown). Hydrogen bonds are shown with thin lines. The O−H hydrogen bond distances are 2.64 and 1.74 Å for the B-1,4 and G-1,3 environments, respectively.

hydrogen bonding, making the zeolite oxygen atom flexible. The alternative model of the G-1,3 environment (G-1,3f) fixed the zeolite oxygen atom involved in the hydrogen bond at its crystallographic position. The adsorption energy of NO varied by only a few kilojoules per mole on these alternative clusters compared to their counterparts, which indicates that the original clusters are sufficiently large to describe the adsorption of molecules that do not form secondary bonds with the zeolite. The adsorption energies of NH_3 and H_2O were not significantly affected by the addition to the B-1,4 cluster, indicating the hydrogen bonding is relatively weak for the B-1,4 environment. However, unlike the extended B-1,4 environment, the energetics of ammonia and water adsorption did change for the G-1,3f cluster (Table 4).

The overall adsorption energies of ammonia and, to a lesser extent, water are actually similar for both treatments of the G-1,3 environment. However, ΔE_{bond} for G-1,3f is less negative than G-1,3 for both adsorbates and considerably so for water. The shift in the bond energies is partially offset by a decrease in ΔE_{strain}. For both molecules, the differences between the G-1,3f environment and the B-1,4 environment are more consistent with the other adsorbates than the G-1,3 environment (Table 5): the ammonia bond energy difference is 8 kJ/mol, which is similar to the average intrinsic preference for the B-1,4 environment of ~13 kJ/mol, while the water bond energy difference is − 3 kJ/mol. The changes in the adsorption energies due to constraining the zeolite oxygen atom in the G environment thus identify another characteristic of preferential adsorption for molecules capable of forming hydrogen bonds: the formation of a

TABLE 5: Difference of G-1,3 and B-1,4 Ammonia and Water Adsorption Energies (kJ/mol)[a]

	environments	$\Delta(\Delta E_{ads})$	$\Delta(\Delta E_{bond})$	$\Delta(\Delta E_{strain})$
$Co-NH_3$	G-1,3/B-1,4	16	−5	23
$Co-NH_3$	G-1,3f/B-1,4	20	8	13
$Co-OH_2$	G-1,3/B-1,4	−3	−39	37
$Co-OH_2$	G-1,3f/B-1,4	10	−3	14

[a] In some cases, the sum of $\Delta(\Delta E_{bond})$ and $\Delta(\Delta E_{strain})$ may not exactly equal $\Delta(\Delta E_{ads})$ due to rounding errors.

secondary hydrogen bond may be more favorable in one environment than another. It should also be noted that the hydrogen-bonded oxygen atom in the G-1,3 environment is coordinated to an aluminum atom, while the corresponding oxygen atom in the B-1,4 environment is not.

The second way in which ammonia and water differ from the other molecules is that they have gas-phase dipoles about an order of magnitude larger than any of the other adsorbates.[28] The long-range electrostatic interactions should therefore be more significant for these two adsorbates. The electrostatic interaction between the adsorbates and the two zeolite clusters was estimated in a simple way with use of Coulomb's law:

$$\Delta E_{\text{Coulomb}} = \sum_i \sum_j \frac{q_i q_j}{4\pi\epsilon_0 r_{ij}} \tag{5}$$

where i refers to the cobalt−zeolite atoms and j to the adsorbate atoms, q is the Mulliken partial charge, ϵ_0 is the vacuum permittivity, and r_{ij} is the distance between atoms i and j. Comparing the results in Tables 1 and 2 for the other adsorbates to those in Table 4 for ammonia and water shows that the Coulomb interaction of ammonia or water with the cobalt−zeolite is considerably larger than that for the other adsorbates. Water, with the larger dipole, has a more significant Coulomb interaction than ammonia. The Coulomb interaction is generally stronger for the G-1,3 environment than the B-1,4 environment, although without including more of the zeolite crystal, we cannot be certain if this is a general property. However, if the electrostatic interactions are indeed more favorable in the G environment than in the B environment, then this could be a fourth characteristic of preferential adsorption that primarily affects polar molecules. Using an embedded cluster approach, Brändle and Sauer[29] determined that 35% of the heat of ammonia adsorption in H-faujasite is due to long-range interactions. Although the clusters used in this investigation are large compared to most other studies (e.g. ref 13), they are still not large enough to fully describe the adsorption of ammonia and water. We have partially accounted for the secondary bond formed by the adsorbate and the zeolite within our current cluster models. However, the long-range electrostatic effects may be significant for these two adsorbates and should be included in future studies with embedding techniques.

Conclusions

The dependence of the NO_x SCR activity on the cobalt loading in zeolites is well-known. The calculations detailed here show that the adsorption of molecules closely related to NO_x reduction chemistry depends on the local zeolite environment. For nearly all of the molecules examined here, adsorption is preferred on cobalt in the B ferrierite environment over cobalt in the G ferrierite environment. This preference arises primarily from two metal−zeolite properties. First, cobalt is more coordinatively unsaturated in the B environment than the G environment. As a result, adsorption is intrinsically favored by

∼13 kJ/mol to cobalt in the B environment. The second characteristic is related to the strain that the adsorbate places on the cobalt−zeolite structure. Adsorbates pull cobalt away from the zeolite to different degrees. The two characteristics usually act in the same direction, making the B environment even more preferred for adsorption. However, in some cases, the strain effect reverses and negates the intrinsic preference of molecules for cobalt in the B environment. Ammonia and water deviate from the trends observed for the other molecules. Both of these molecules form a secondary hydrogen bond with the zeolite; hydrogen bond formation for water and ammonia is more favorable in the G environment than the B environment. Additionally, long-range electrostatic forces in the zeolite are expected to more significantly affect ammonia and water than the other adsorbates. The electrostatic contribution to adsorption was estimated to be larger for the G environment than for the B environment.

Acknowledgment. This work was supported by the EMSI program of the National Science Foundation and the Department of Energy (CHE-9810378) at the Northwestern University Institute for Environmental Catalysis. Additional support was provided by the National Computational Science Alliance (CTS010016N) utilizing the NCSA Origin 2000.

Supporting Information Available: The Cartesian coordinates of all the zeolite clusters. This material is available free of charge via the Internet at http://pubs.acs.org.

References and Notes

(1) Traa, Y.; Burger, B.; Weitkamp, J. *Microporous Mesoporous Mater.* **1999**, *30*, 3−41.
(2) Li, Y.; Armor, J. N. *Appl. Catal. B* **1992**, *1*, L31−40.
(3) Armor, J. N. *Catal. Today* **1995**, *26*, 147−158.
(4) Li, Y.; Armor, J. N. *J. Catal.* **1994**, *150*, 376−387.
(5) Li, Y.; Slager, T. L.; Armor, J. N. *J. Catal.* **1994**, *150*, 388−399.
(6) El-Malki, E.-M.; Werst, D.; Doan, P. E.; Sachtler, W. M. H. *J. Phys. Chem. B* **2000**, *104*, 5924−5931.
(7) Wang, X.; Chen, H.-Y.; Sachtler, W. M. H. *Appl. Catal. B* **2000**, *26*, L227-L239.
(8) Wang, X.; Chen, H.; Sachtler, W. M. H. *Appl. Catal. B* **2001**, *29*, 47−60.
(9) Kaucký, D.; Vondrová, A.; Dědeček, J.; Wichterlová, B. *J. Catal.* **2000**, *194*, 318−329.
(10) Kaucký, D.; Dědeček, J.; Wichterlová, B. *Microporous Mesoporous Mater.* **1999**, *31*, 75−87.
(11) Mortier, W. J. *Compilation of Extra Framework Sites in Zeolites*; Butterworth Scientific: London, UK, 1982.
(12) Sengupta, D.; Adams, J. B.; Schneider, W. F.; Hass, K. C. *Catal. Lett.* **2001**, *74*, 193−199.
(13) Ryder, J. A.; Chakraborty, A. K.; Bell, A. T. *J. Phys. Chem. B* **2002**, *106*, 7059−7064.
(14) Solans-Monfort, X.; Branchadell, V.; Sodupe, M. *J. Phys. Chem. B* **2002**, *106*, 1372−1379.
(15) Nachtigallová, D.; Nachtigall, P.; Sauer, J. *Phys. Chem. Chem. Phys.* **2001**, *3*, 1552−1559.
(16) Pierloot, K.; Delabie, A.; Groothaert, M. H.; Schoonheydt, R. A. *Phys. Chem. Chem. Phys.* **2001**, *3*, 2174−2183.
(17) Delabie, A.; Pierloot, K.; Groothaert, M. H.; Weckhuysen, B. M.; Schoonheydt, R. A. *Phys. Chem. Chem. Phys.* **2002**, *4*, 134−145.
(18) McMillan, S. A.; Broadbelt, L. J.; Snurr, R. Q. *J. Phys. Chem. B* **2002**, *106*, 10864−10872.
(19) Barbosa, L. A. M. M.; Zhidomirov, G. M.; van Santen, R. A. *Phys. Chem. Chem. Phys.* **2000**, *2*, 3909−3918.
(20) Barbosa, L. A. M. M.; van Santen, R. A.; Hafner, J. *J. Am. Chem. Soc.* **2001**, *123*, 4530−4540.
(21) Barbosa, L. A. M. M.; Zhidomirov, G. M.; van Santen, R. A. *Catal. Lett.* **2001**, *77*, 55−62.
(22) McMillan, S. A.; Broadbelt, L. J.; Snurr, R. Q. *J. Catal.* **2003**, *219*, 117−125.
(23) Davidová, M.; Nachtigallová, D.; Bulánek, R.; Nachtigall, P. *J. Phys. Chem. B* **2003**, *107*, 2327−2332.
(24) Sobalík, Z.; Dědeček, J.; Wichterlová, B.; Drozdová, L.; Prins, R. *J. Catal.* **2000**, *194*, 330−342.
(25) Frisch, M. J.; Trucks, G. W.; Schlegel, H. B.; Scuseria, G. E.; Robb, M. A.; Cheeseman, J. R.; Zakrzewski, V. G.; Montgomery, J. A., Jr.; Stratmann, R. E.; Burant, J. C.; Dapprich, S.; Millam, J. M.; Daniels, A. D.; Kudin, K. N.; Strain, M. C.; Farkas, O.; Tomasi, J.; Barone, V.; Cossi, M.; Cammi, R.; Mennucci, B.; Pomelli, C.; Adamo, C.; Clifford, S.; Ochterski, J.; Petersson, G. A.; Ayala, P. Y.; Cui, Q.; Morokuma, K.; Rega, N.; Salvador, P.; Dannenberg, J. J.; Malick, D. K.; Rabuck, A. D.; Raghavachari, K.; Foresman, J. B.; Cioslowski, J.; Ortiz, J. V.; Baboul, A. G.; Stefanov, B. B.; Liu, G.; Liashenko, A.; Piskorz, P.; Komaromi, I.; Gomperts, R.; Martin, R. L.; Fox, D. J.; Keith, T.; Al-Laham, M. A.; Peng, C. Y.; Nanayakkara, A.; Challacombe, M.; Gill, P. M. W.; Johnson, B.; Chen, W.; Wong, M. W.; Andres, J. L.; Gonzalez, C.; Head-Gordon, M.; Replogle, E. S.; Pople, J. A. *Gaussian 98*, Revision A.11.3; Gaussian, Inc.: Pittsburgh, PA, 2002.
(26) Hoffmann, R. *Solids and Surfaces: A Chemist's View of Bonding in Extended Structures*; VCH: New York, 1988.
(27) Lee, W. T.; Ford, L.; Blowers, P.; Nigg, H. L.; Masel, R. I. *Surf. Sci.* **1998**, *416*, 141−151.
(28) Weast, R. C.; Astle, M. J.; Beyer, W. H., Eds. *CRC Handbook of Chemistry and Physics*, 67th ed.; CRC Press: Boca Raton, FL, 1987.
(29) Brändle, M.; Sauer, J. *J. Mol. Catal. A-Chem.* **1997**, *119*, 19−33.